ACS SENSORS

pubs.acs.org/acssensors

Article

Mutant Flavin-Based Fluorescent Protein Sensors for Detecting Intracellular Zinc and Copper in *Escherichia coli*

Wenping Zou, Hazel N. Nguyen, and Melissa L. Zastrow*

Cite This: *ACS Sens.* 2022, 7, 3369−3378

Read Online

ACCESS | Metrics & More | Article Recommendations | Supporting Information

ABSTRACT: Flavin-based fluorescent proteins (FbFPs) are a class of fluorescent reporters that undergo oxygen-independent fluorophore incorporation, which is an important advantage over green fluorescent proteins (GFPs) and mFruits. A FbFP derived from *Chlamydomonas reinhardtii* (CreiLOV) is a promising platform for designing new metal sensors. Some FbFPs are intrinsically quenched by metal ions, but the question of where metals bind and how to tune metal affinity has not been addressed. We used site-directed mutagenesis of CreiLOV to probe a hypothesized copper(II) binding site that led to fluorescence quenching. Most mutations changed the fluorescence quenching level, supporting the proposed site. One key mutation introducing a second cysteine residue in place of asparagine ($CreiLOV_{N41C}$) significantly altered metal affinity and selectivity, yielding a zinc sensor. The fluorescence intensity and lifetime of $CreiLOV_{N41C}$ were reversibly quenched by Zn^{2+} ions with a biologically relevant affinity (apparent dissociation constant, K_d, of 1 nM). Copper quenching of $CreiLOV_{N41C}$ was retained but with several orders of magnitude higher affinity than CreiLOV (K_d = 0.066 fM for Cu^{2+}, 5.4 fM for Cu^{+}) and partial reversibility. We also show that $CreiLOV_{N41C}$ is an excellent intensity- and lifetime-based zinc sensor in aerobic and anaerobic live bacterial cells. Zn^{2+}-induced fluorescence quenching is reversible over several cycles in *Escherichia coli* cell suspensions and can be imaged by fluorescence microscopy. $CreiLOV_{N41C}$ is a novel oxygen-independent metal sensor that significantly expands the current fluorescent protein-based toolbox of metal sensors and will allow for studies of anaerobic and low oxygen systems previously precluded by the use of oxygen-dependent GFPs.

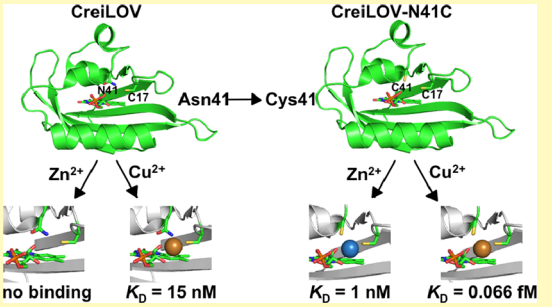

KEYWORDS: *flavin-based fluorescent protein, fluorescent metal sensor, anaerobic, bacteria, zinc, copper, genetically encoded, fluorescence lifetime*

Transition metals like zinc are essential elements for life and, as cofactors of proteins, play crucial roles in catalysis, structural stabilization, and signaling.[1] One approach to studying the functions of metal ions in biological systems is to use optical sensors, which can detect, quantify, and track metals in concentration ranges that match the affinity of a given sensor.[2] Genetically encoded sensors based on green fluorescent proteins (GFPs) and their derivatives are frequently used for metal ion detection.[3−6] Broadly, GFPs can serve as single fluorescent protein-based sensors with an attached or embedded metal binding site that modulates fluorescence in response to the analyte or can be a component of multi-fluorescent protein-based probes employing a metal-dependent Förster resonance energy transfer (FRET) mechanism. The toolbox of GFP-based sensors is a cornerstone for studying metals in biology, yet GFPs have limitations that prevent widespread use. GFP-based sensors cannot be readily applied under anaerobic or hypoxic conditions because oxygen is required for the maturation of the *p*-hydroxybenzylidene chromophore and resultant fluorescence activation.[7,8]

Efforts to develop new biomolecular reporters for studying low oxygen systems like the gut microbiota and other anaerobic bacteria or hypoxic tumors have led to the discovery and development of various cofactor-binding fluorescent protein-based reporters.[9,10] Among these are the flavin mononucleotide (FMN)-binding proteins.[11,12] Flavin-based fluorescent proteins (FbFPs) are derived from blue light receptors known as light, oxygen, or voltage (LOV) sensing proteins.[13] Native LOV proteins are nonfluorescent by virtue of their photochemistry, which is used to couple photoexcitation with electronic and structural changes in the protein. Mutation of a photoactive cysteine residue to alanine impairs the native photocycle and results in a fluorescence mechanism that does not rely on oxygen.[14,15] FbFPs are therefore suitable and now well-demonstrated reporters for use in anaerobic organisms.[16−21] The LOV domain found in fresh water algae, *Chlamydomonas reinhardtii* (CreiLOV), shows a relatively high quantum yield (∼0.51) and brightness among the LOV

Received: June 28, 2022
Accepted: October 14, 2022
Published: October 25, 2022

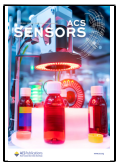

proteins.[22] Other advantages include high thermal stability and fluorescence over a wide range of pH values from 3 to 11, making CreiLOV an excellent candidate reporter for spectroscopic imaging applications, including metal detection.

Previous work found that the FbFP iLOV can be quenched by Cu^{2+} (apparent dissociation constant, K_d = 4.72 μM at pH 7.4) and other FbFP mutants are sensitive to Hg^{2+} and As^{3+} ions, although none of these FbFPs were tested in live cells.[23−25] Our group found that Cu^{2+} induces quenching of CreiLOV with a slightly stronger binding affinity (K_d = 3.2 ± 0.3 μM) than iLOV and can detect excess Cu^{2+} ions added to *Escherichia coli* cells.[26] Both iLOV and CreiLOV dissociation constants were obtained by direct titration with Cu^{2+}, an approach that we have since shown is not suitable for this metal under neutral buffered conditions and can underestimate the affinity.[27] A copper binding site was proposed within the FMN binding pocket.[23,26] In CreiLOV, copper may coordinate with Cys17 and Asn41 (Figures 1A,B and S1), and in iLOV,

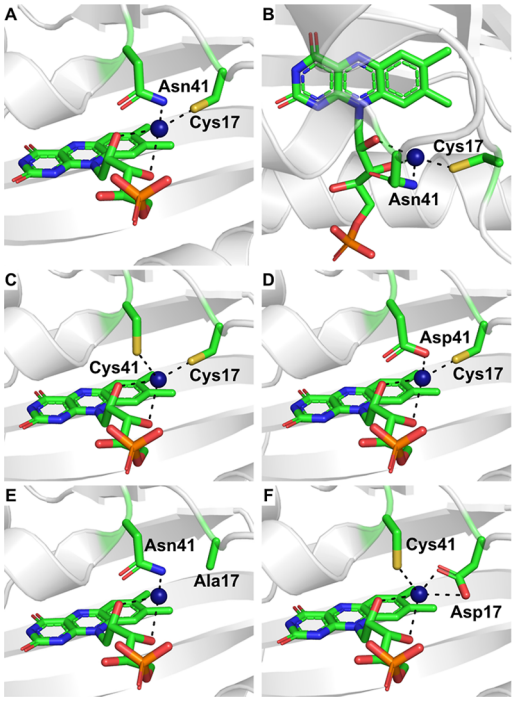

Figure 1. Models of metal binding sites in CreiLOV and CreiLOV mutants. (A,B) Different views of the proposed metal binding site in CreiLOV (based on PDB 1N9L). (C−F) Proposed metal binding sites in CreiLOV mutants (C) N41C, (D) N41D, (E) C17A, and (F) C17D, N41C. Models were made in PyMOL with the metal added manually. The flavin cofactor and side chains that make up the proposed binding site are colored green. The modeled metal ion (copper or zinc) is shown in blue.

these residues are Asn17 and Asn41. Copper may also coordinate directly to two oxygen atoms on the FMN cofactor, and a coordinating solvent molecule could be present. Although CreiLOV was demonstrated to respond to Cu^{2+} in live *E. coli* cells, the low binding affinity reported at the time (micromolar K_d) makes studying microorganism metal levels challenging because free or detectable copper concentrations are estimated to be below femtomolar and in bacteria are likely in the attomolar range, although this could vary between different species.[28,29] Here, by titration in the presence of suitable chelators, we show that the affinity previously reported was an underestimate of the actual stronger affinity (K_d ~ 0.1 nM). This dissociation constant, however, remains lower than the levels of detectable copper expected in cells.

In this work, we aimed to create an oxygen-independent protein-based sensor with high metal affinity that could be used to detect metal ions in anaerobic organisms. We hypothesized that the metal binding affinity and copper-induced quenching could be tuned via mutagenesis of the coordinating amino acids in CreiLOV (Figure 1). Here, we tested this hypothesis using site-directed mutagenesis on the amino acids at positions 17 and 41. We show that mutating position 17 to Ala to remove the coordinating Cys residue decreases the extent of copper quenching. The $CreiLOV_{N41D}$ mutant shows similar results. Exchanging the position of Cys17 with Asn41 and mutating position 17 to Asp led to the loss of FMN binding and fluorescence. Mutating position 41 to Cys, however, led to a significant increase in affinity for copper (subfemtomolar K_d) and introduced a nanomolar K_d for and reversible quenching response to Zn^{2+}. In bacteria, zinc is buffered in the nanomolar to picomolar range, making this mutant well suited for bacterial zinc detection.[28,30] We describe how $CreiLOV_{N41C}$ can probe Cu^{2+}, Cu^{+}, which is the predominant redox state within bacterial cells, and Zn^{2+}. Fluorescence can be successively and rapidly quenched and recovered with no loss in fluorescence for Zn^{2+} within bacterial cells grown under aerobic and anaerobic conditions. For copper, fluorescence can be partially recovered. Given the complete reversibility of CreiLOV with zinc, we focus on demonstrating the utility of CreiLOV for exogenous and endogenous zinc detection in cells under aerobic and anaerobic conditions. The results support the previously proposed copper binding site in CreiLOV. More importantly, we have developed a fluorescent protein-based zinc sensor that can be used to detect zinc reversibly under anaerobic conditions, for which studies were previously precluded by the oxygen dependence of GFP-derived fluorescent protein-based sensors.

RESULTS AND DISCUSSION

Construction, Expression, and Characterization of CreiLOV Mutants. CreiLOV mutants (Figure 1C−F) were prepared by site-directed mutagenesis (primers in Table S1) and expressed in *E. coli* separately. After purification, gel electrophoresis reflected the monomeric form of each denatured mutant except $CreiLOV_{N41C}$, for which a potentially aberrant disulfide bond was formed (Figure S2). Purified $CreiLOV_{N41C}$ was treated with reductant prior to characterization. The spectroscopic properties of all purified proteins are similar (Figures 2A and S3, Table S2).

Several biologically relevant metal ions were screened to determine the effects on the fluorescence of each CreiLOV mutant and for comparison to CreiLOV. Previously, we measured 64% quenching of CreiLOV by Cu^{2+}.[26] Here, we also investigated Cu^{+}, as the predominant intracellular form of copper, and found 75% fluorescence quenching (Table 1). For $CreiLOV_{N41C}$, Cu^{+} induced 97% quenching and Cu^{2+} induced a 91% decrease in fluorescence intensity (Table 1, Figure 2B). The extent of fluorescence quenching by copper was somewhat reduced for mutants $CreiLOV_{C17A}$ (54% by Cu^{2+} and 43% by Cu^{+}) and $CreiLOV_{N41D}$ (59% by Cu^{2+} and 56% by Cu^{+}) (Table 1, Figure 2C,D). As for CreiLOV, Zn^{2+} and Cd^{2+} induced only minor intensity quenching for CreiLOV mutants except $CreiLOV_{N41C}$, for which 95% quenching of the

https://doi.org/10.1021/acssensors.2c01376
ACS Sens. 2022, 7, 3369−3378

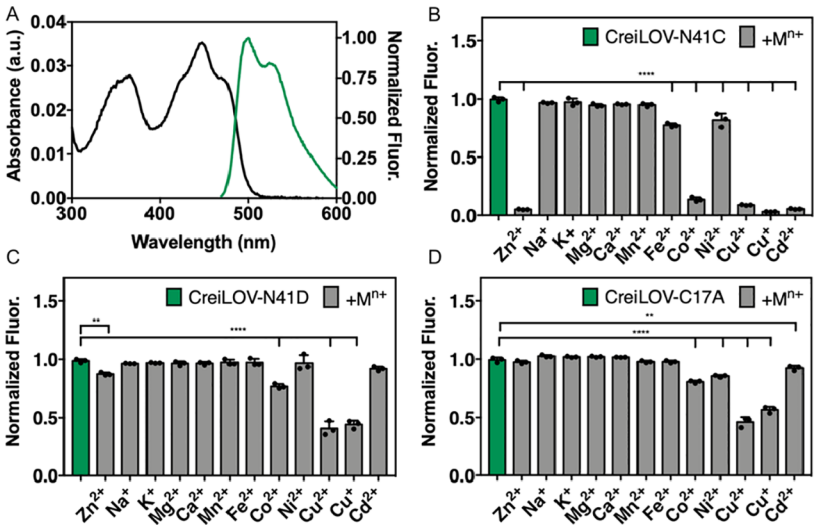

Figure 2. UV−visible and fluorescence properties of CreiLOV mutants. (A) UV−visible (black line) and normalized fluorescence emission (green line) spectra of $CreiLOV_{N41C}$. Metal sensitivity of (B) $CreiLOV_{N41C}$, (C) $CreiLOV_{N41D}$, and (D) $CreiLOV_{C17A}$. To 3 μM of protein, 266 equiv (Na^+, K^+, Mg^{2+}, or Ca^{2+}) or 33 equiv (Cu^+, Cu^{2+}, Zn^{2+}, Cd^{2+}, Co^{2+}, Mn^{2+}, Ni^{2+}, or Fe^{2+}) metal salt was added. Data are shown as normalized emission at 497 nm. λ_{ex} = 450 nm. Buffer: 50 mM HEPES, 100 mM NaCl, pH 7.1. Data were analyzed by means of one-way analysis of variance; $^{**}p < 0.005$, $^{***}p < 0.001$, $^{****}p < 0.0001$. Individual data points are overlaid on the bar chart representation. All error bars represent the standard deviation for three replicates.

Table 1. Fluorescence Quenching and Metal Binding Affinities of CreiLOV and CreiLOV Mutants

protein	% quenched by Zn^{2+}	K_d for Zn^{2+} (M)	% quenched by Cu^+	K_d for Cu^+ (M)[a]	% quenched by Cu^{2+}	K_d for Cu^{2+} (M)
CreiLOV	16 ± 2	N.A.	75 ± 5	$1.2(0.1) \times 10^{-5}$	64 ± 3	$1.5(0.1) \times 10^{-10}$
$CreiLOV_{C17A}$	3 ± 1	N.A.	43 ± 3	$6(2) \times 10^{-5}$	54 ± 4	$1.1(0.1) \times 10^{-10}$
$CreiLOV_{N41C}$	95 ± 1	$1.0(0.2) \times 10^{-9}$	97 ± 1	$5.4(0.6) \times 10^{-15}$	91 ± 1	$6.6(1.7) \times 10^{-17}$
$CreiLOV_{N41D}$	13 ± 1	N.A.	56 ± 3	$2.1(0.4) \times 10^{-5}$	59 ± 6	$1.1(0.2) \times 10^{-10}$

[a]Data collected by direct titration with $[Cu(CH_3CN)_4]PF_6$ for all mutants except $CreiLOV_{N41C}$. Dissociation constants therefore represent the upper limits for Cu^+ binding.

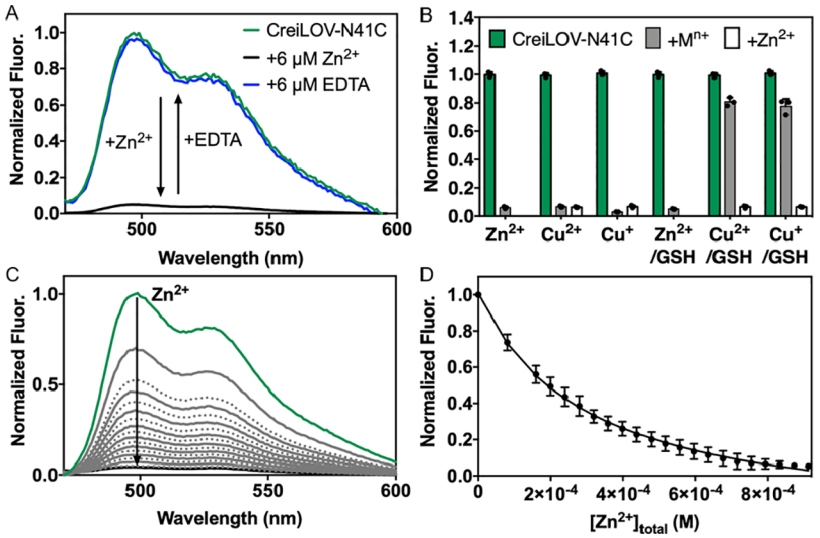

Figure 3. $CreiLOV_{N41C}$ and Zn^{2+} binding studies. (A) Reversibility of Zn^{2+} binding to $CreiLOV_{N41C}$ was detected by the change in fluorescence emission. (B) Selectivity of $CreiLOV_{N41C}$ for Zn^{2+} in the absence and presence of GSH (2 mM). To $CreiLOV_{N41C}$ (3 μM), $CuCl_2$ or $[Cu(CH_3CN)_4]PF_6$ (100 μM) was added, followed by $ZnCl_2$ (100 μM). Individual data points are overlaid on the bar chart representation. (C) Normalized fluorescence spectra of $CreiLOV_{N41C}$ (3 μM) titrated with increasing amounts of $ZnCl_2$ in the presence of EGTA (1 mM). (D) Integrated fluorescence from part C plotted against total Zn^{2+} concentration. Fluorescence is normalized relative to the initial $CreiLOV_{N41C}$ fluorescence. Data was fitted with DynaFit (Experimental Section). Buffer: 50 mM HEPES, 100 mM NaCl, pH 7.1. λ_{ex} = 450 nm. All error bars represent the standard deviation for three replicates.

https://doi.org/10.1021/acssensors.2c01376
ACS Sens. 2022, 7, 3369−3378

fluorescence intensity was observed (Table 1, Figure 2B). All other metals induced little to no quenching for CreiLOV$_{N41C}$ except Fe^{2+} (23%), Co^{2+} (86%), and Ni^{2+} (18%). Co^{2+} and Ni^{2+} showed up to 20% quenching for the other two mutants CreiLOV$_{N41D}$ (Co^{2+} only) and CreiLOV$_{C17A}$ (Figure 2C,D). The proposed metal binding site in CreiLOV$_{N41C}$, which includes two Cys residues together with FMN, likely contributes to the change in metal ion response. By contrast, CreiLOV and CreiLOV$_{N41D}$ each have only one Cys residue and CreiLOV$_{C17A}$ does not have any nearby Cys residues.

Given the substantial response to Zn^{2+} and $Cu^{+/2+}$ by CreiLOV$_{N41C}$, we sought to better understand its potential as a zinc and copper sensor. First, we investigated the effects of each metal on the absorption spectrum of CreiLOV$_{N41C}$ (Figure S4). Zn^{2+} did not change the absorption spectrum of CreiLOV$_{N41C}$. Both Cu^{+} and Cu^{2+} increased the intensity of the peak at 270 nm, which is consistent with a copper metal thiolate charge-transfer band similar to those found in the reported proteins.[31,32] Examination of the effects of biologically relevant nonmetal ions shows little influence on the emission of CreiLOV$_{N41C}$ (Figure S5). We also tested the reversibility of zinc- and copper-induced changes in the fluorescence intensity. The emission intensity quenched by Zn^{2+} could be fully restored with the addition of ethylenediaminetetraacetic acid (EDTA, Figure 3A). The intensity quenched by Cu^{+} or Cu^{2+} could be restored to 80% of the original level by the addition of *N*,*N*,*N*′,*N*′-tetrakis(2-pyridylmethyl)ethylenediamine (TPEN) for Cu^{2+} (Figure S6A,B) or dithiothreitol (DTT) for Cu^{+} (Figure S6C,D). Given that only zinc quenching was completely reversible, we carried out additional characterizations focused on zinc. Zn^{2+}-induced quenching from pH 5.5 to 8.5 was tested, and substantial quenching from pH 6.5 and above was observed (Figure S7). The kinetics of zinc-induced fluorescence intensity quenching (k_{quench} = 0.44 s^{-1}; $t_{1/2}$ = 1.57 s) and EDTA-mediated recovery ($k_{reverse}$ = 0.096 s^{-1}; $t_{1/2}$ = 7.23 s) for pure CreiLOV$_{N41C}$ were measured and are rapid (Table S3, Figure S8A,B). Given that CreiLOV$_{N41C}$ could be quenched by both zinc and copper, we sought to understand if the mutant showed any selectivity. Under standard buffered conditions, selectivity for copper was found (Figures 3B and S9). In cells, however, high concentrations of other molecules are present. For example, the reducing intracellular environment of live cells is maintained with the help of enzymatic or nonenzymatic antioxidants, like glutathione (GSH, often millimolar levels).[33,34] Given that GSH binds copper tightly, its presence in aqueous buffer can induce the selectivity of CreiLOV$_{N41C}$ toward Zn^{2+} (Figure 3B).[35]

Copper and Zinc Binding Affinities of CreiLOV Mutants. Next, we investigated the affinity of CreiLOV$_{N41C}$ for each metal to determine the concentration ranges in which the sensor could be useful. To determine the affinity of CreiLOV$_{N41C}$ toward Zn^{2+}, titrations were set up using metal buffering systems to allow the control of labile Zn^{2+} concentrations (Table S4). Among several chelators tested, ethylene glycol-bis(β-aminoethyl ether)-*N*,*N*,*N*′,*N*′-tetraacetic acid (EGTA) worked best for CreiLOV$_{N41C}$. Titration of CreiLOV$_{N41C}$ in the presence of EGTA with increasing Zn^{2+} led to a binding isotherm with decreasing fluorescence that could be fitted to a single site binding model (K_d = 1.0 ± 0.2 nM (Table 1, Figure 3C). By comparison, no significant Zn^{2+} binding was detected for CreiLOV, CreiLOV$_{C17A}$, or CreiLOV$_{N41D}$. The nanomolar K_d falls into the range of physiologically relevant labile zinc concentrations found in biological systems, including bacteria.[28,30] CreiLOV$_{N41C}$ would therefore be a valuable addition to the current collection of genetically encoded protein-based zinc sensors, many of which are based on the oxygen-dependent GFPs.[6,36−50] Because CreiLOV$_{N41C}$ does not require oxygen to become fluorescent, it may be applied in biological systems where GFPs are generally unsuitable, such as the gut microbiota.

The Cu^{2+} binding affinity for CreiLOV$_{N41C}$ was determined by buffering Cu^{2+} concentrations to the subfemtomolar level using EDTA (Table S4). The single site K_d of CreiLOV$_{N41C}$ for Cu^{2+} is 0.07 ± 0.02 fM (Figure S10A). By comparison, the Cu^{2+} affinities measured in the presence of a chelator for CreiLOV and the other CreiLOV mutants were several orders of magnitude weaker (Table 1). Previously, we reported a Cu^{2+} K_d of 3.2 μM for CreiLOV, which was measured by direct titration with up to 100 μM Cu^{2+}, similar to the approach used for measuring the Cu^{2+} affinities of several other fluorescent proteins quenched by copper.[23,26,51−55] At physiological pH, however, copper has a solubility of only ∼2 μM, which could lead to an underestimation of copper affinity. Upon revisiting the measurement of the Cu^{2+} affinity in the presence of *N*-(2-carboxyethyl)iminodiacetic acid (ADA) to buffer Cu^{2+} to subnanomolar levels, a K_d of 0.15 nM was obtained. Similarly, subnanomolar dissociation constants of Cu^{2+} were found for CreiLOV$_{C17A}$ and CreiLOV$_{N41D}$ (Tables 1 and S4, Figure S11). These results are similar to those that we recently reported for Cu^{2+} quenching of near-infrared fluorescent proteins, where a picomolar Cu^{2+} K_d was determined with nitrilotriacetic acid (NTA) present, but micromolar K_d values were found using the direct titration method.[27]

We also measured the Cu^{+} affinity for each mutant. For CreiLOV$_{N41C}$, the Cu^{+} concentration was buffered to the femtomolar level with GSH (Table S4). The resulting binding isotherm could be fitted to a single site binding model accounting for the chelator to give a K_d of 5.4 ± 0.6 fM (Figure S10B). For CreiLOV, CreiLOV$_{C17A}$, and CreiLOV$_{N41D}$, we tried several available Cu^{+} chelators, all of which were too strong for reaching a suitable binding equilibrium.[35,56] Therefore, we used a direct titration method for Cu^{+} to estimate an upper limit to the dissociation constant of ∼10−60 μM (Table 1, Figure S12). These K_d values are likely underestimates due to the precipitation of Cu^{+}. The chelators tested include DTT (K_d = 5.01 × 10^{-16} M), GSH (K_d = 5.01 × 10^{-14} M), and cysteine (K_d = 1.25 × 10^{-10} M) to buffer the Cu^{+} concentration, but even the weakest (cysteine) with subnanomolar binding was too strong for these CreiLOV variants.[35,56] Compared to CreiLOV, CreiLOV$_{C17A}$, and CreiLOV$_{N41D}$, the 6−10 orders of magnitude higher affinity for $Cu^{+/2+}$ of CreiLOV$_{N41C}$ suggests that coordination involves both Cys17 and Cys41.

Fluorescence Lifetimes of CreiLOV Mutants. FbFPs like CreiLOV tend to have relatively long fluorescence lifetimes, making them excellent candidates for lifetime-based detection methods using single- or multi-protein platforms. The lifetime of CreiLOV is 4.5 ns, which fits in the range from 3 to 6 ns measured for most FbFPs.[26,57,58] Here, we found that all of the CreiLOV mutant lifetimes remained around 4.5 ns (Table S2). Previously, we showed that Cu^{2+} could decrease the lifetime of CreiLOV by ∼50%.[26] Here, addition of excess Zn^{2+} decreases the lifetime of CreiLOV$_{N41C}$ to 2.7 ns and can be reversed to the original level with 1 equiv of EDTA (Figure S13). In the presence of excess Cu^{2+}, the lifetime of CreiLOV$_{N41C}$ was decreased, albeit to a lesser extent (3.6

https://doi.org/10.1021/acssensors.2c01376
ACS Sens. 2022, 7, 3369−3378

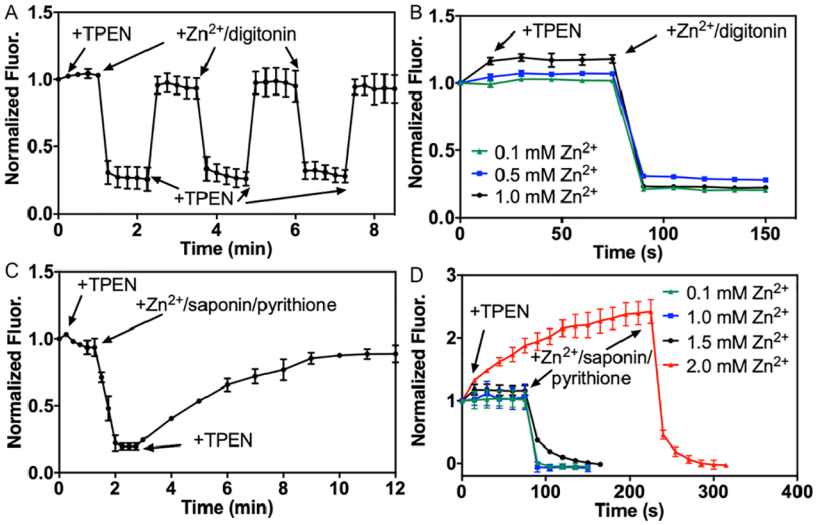

Figure 4. Fluorescence studies of Zn^{2+}-induced quenching of CreiLOV$_{N41C}$ in live *E. coli* cell suspensions. (A) Fluorescence emission was recorded under aerobic conditions initially and every 15 s after the addition of the intracellular chelator TPEN (50 μM) or $ZnCl_2$/digitonin (100 μM/30 μM). A total of three cycles of zinc quenching and reversal with chelator were recorded. (B) Changes in endogenous zinc were detected by measuring the fluorescence emission of *E. coli* cells grown in the presence of 0.1, 0.5, or 1 mM $ZnCl_2$ (aerobic conditions) initially and every 15 s after the addition of TPEN (50 μM) and then $ZnCl_2$/digitonin (100 μM/30 μM). (C) Fluorescence emission was recorded under anaerobic conditions initially and every 15 s after an initial addition of the TPEN (50 μM), followed by $ZnCl_2$/saponin/pyrithione (100 μM/0.001%/0.75 μM). Then, excess TPEN (200 μM) was added, and fluorescence was recorded every 1 min. D) Changes in endogenous zinc under anaerobic conditions were detected by measuring the fluorescence emission of *E. coli* cells grown in the presence of 0.1, 1.0 mM, 1.5 mM, or 2.0 mM $ZnCl_2$ initially and every 15 s after the addition of TPEN (50 μM) and $ZnCl_2$/saponin/pyrithione (100 μM/0.001%/0.75 μM for 0.1 and 1.0 mM $ZnCl_2$ or 100 μM/0.002%/1.5 μM for 1.5 and 2.0 mM $ZnCl_2$). Buffer: 50 mM HEPES, 100 mM NaCl, pH 7.1. λ_{ex} = 450 nm. All error bars represent the standard deviation for three replicates. Then, excess Zn^{2+} along with digitonin was added to yield the fluorescence intensity of fully zinc-bound CreiLOV$_{N41C}$. As the concentration of zinc present in the growth medium increased, the extent of initial quenching was higher, suggesting an increase in endogenous zinc in the cells that could be detected with CreiLOV$_{N41C}$.

ns), and was mostly reversed (4.3 ns) using excess TPEN (Figure S14A,B). Similarly, excess Cu^+ reduced the lifetime to 3.3 ns and excess DTT reversed it to 4.2 ns (Figure S14C,D).

Metal-Induced Fluorescence Quenching of CreiLOV$_{N41C}$ in Aerobic and Anaerobic Live Bacterial Cells. To test whether CreiLOV$_{N41C}$ could be a useful zinc sensor in living systems, we monitored the fluctuation of Zn^{2+} ions in live *E. coli* cells using the change in fluorescence signal. Specifically, we measured both the fluorescence intensity (Figures 4A and S15) and lifetime (Figure S16) of a live cell suspension of *E. coli* cells that had been transformed and induced to express CreiLOV$_{N41C}$. Compared to the initial signal, little to no change in fluorescence intensity or lifetime occurred with the addition of TPEN. Subsequent addition of Zn^{2+} combined with digitonin to facilitate the cellular uptake of metal resulted in an 80% decrease in fluorescence intensity and a lifetime decrease to 2.6 ns. These results are similar to those observed for the pure protein sample (Figures 3 and S13). Addition of excess TPEN to chelate zinc allows for nearly full recovery of the fluorescence intensity and reversal of the lifetime to 4.2 ns. At least three cycles of zinc-induced quenching and TPEN-facilitated recovery could be achieved, suggesting that CreiLOV$_{N41C}$ is relatively stable in live bacterial cells that contain numerous potential interfering factors not present in aqueous buffer. Furthermore, the kinetics of Zn^{2+}-induced fluorescence intensity quenching (k_{quench} = 0.14 s^{-1}; $t_{1/2}$ = 4.8 s) and TPEN-mediated recovery ($k_{reverse}$ = 0.116 s^{-1}; $t_{1/2}$ = 6.0 s) in live bacterial cells were measured (Table S3, Figure S8C,D). The rapid fluorescence quenching ($t_{1/2}$ < 1 min) induced by zinc in both pure protein (Figure S8A,B) and live bacterial cells highlights the potential of CreiLOV$_{N41C}$ for the detection of rapid zinc fluctuations in living systems.

We further explored the suitability of CreiLOV$_{N41C}$ for measuring zinc in live cells by detecting changes in endogenous zinc levels for *E. coli* grown in the presence of varied zinc concentrations. We focused on zinc here because Zn^{2+}-induced fluorescence quenching of pure protein was completely reversible and the sensor affinity is well suited for detecting physiological zinc levels. Here, *E. coli* cells were grown, and expression of CreiLOV$_{N41C}$ was induced in medium containing 0.1, 0.5, or 1.0 mM $ZnCl_2$ (Figures 4B and S17). The initial fluorescence of each cell suspension was measured, followed by the addition of TPEN to determine the extent of initial quenching that was due to the presence of excess zinc during growth.

We also measured the fluctuation of Cu^+ ions in cells. After measuring the initial fluorescence and the fluorescence upon addition of TPEN, Cu^+ and digitonin were added, and an 80% decrease in fluorescence intensity was measured. Subsequently, up to 80% of the original intensity could be recovered with the addition of TPEN. In contrast to zinc, when multiple quenching and recovery cycles were carried out for Cu^+, the recovered fluorescence intensity decreased after each round. After three quenching-recovery cycles, only 50% of the original intensity was restored after the final TPEN addition (Figure S18). This result is consistent with the incomplete reversibility observed for pure protein (Figure S6C,D).

Next, we used fluorescence microscopy to visualize the zinc-induced fluorescence change in *E. coli* cells expressing CreiLOV$_{N41C}$. The fluorescence signal in the green channel was measured before and after adding an intracellular chelator,

https://doi.org/10.1021/acssensors.2c01376
ACS Sens. 2022, 7, 3369−3378

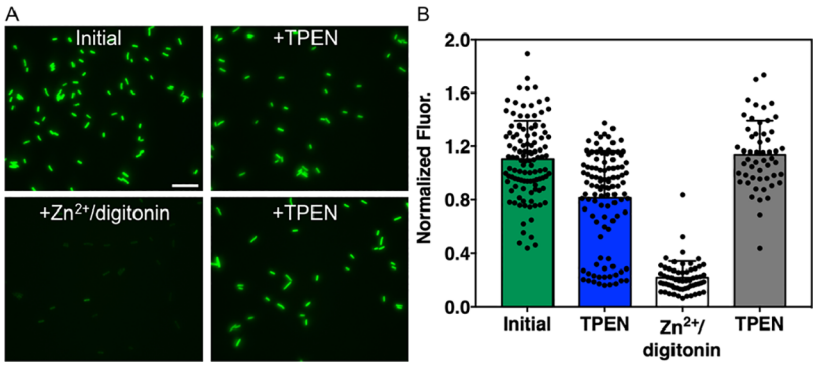

Figure 5. Fluorescence microscopy of *E. coli* cells expressing CreiLOV$_{N41C}$. (A) Top row: fluorescence signal from CreiLOV$_{N41C}$ initially (left) and 1 min after the addition of TPEN (50 μM, right). Bottom row: fluorescence signal 1 min after the addition of Zn^{2+}/digitonin (100 μM/30 μM, left) and 1 min after the addition of TPEN (100 μM, right). Scale bar = 10 μm. (B) Quantification of change in fluorescence signals shown in part A. Mean cell intensities are normalized to the initial intensity. Individual data points are overlaid on the bar chart representation and were collected from three independent experiments. Data were analyzed by means of one-way analysis of variance; ****$p < 0.0001$. Error bars represent the standard deviation.

TPEN. A small signal change was observed over 1 min following the chelator addition, after which no further change was observed. Addition of Zn^{2+}/digitonin quenched the signal, and addition of excess TPEN resulted in near complete signal recovery (Figure 5A,B). The reversibility of Zn^{2+}-induced quenching of CreiLOV$_{N41C}$ as detected by fluorescence imaging is consistent with that measured in cuvettes containing live bacterial cell suspensions, supporting the conclusion that the signal change inside *E. coli* cells is induced by the metal binding to CreiLOV$_{N41C}$.

To analyze whether CreiLOV$_{N41C}$ could be a good zinc sensor in anaerobic living systems, we tested the fluorescence response to Zn^{2+} ions in anaerobically grown live *E. coli* MG1655 cells. Using CreiLOV$_{N41C}$-expressing cell suspensions of *E. coli* grown and maintained under anaerobic conditions, the initial fluorescence intensity was recorded and is similar when compared with the same cell strain grown aerobically and expressing CreiLOV$_{N41C}$ (Figure S19). Addition of TPEN slightly increased the intensity, which then leveled off. Then, addition of Zn^{2+}/saponin/pyrithione induced 80% intensity quenching, and full recovery mediated by TPEN was observed (Figures 4C and S20). This result is similar to the experiment for aerobically grown *E. coli* BL21(DE3) cell suspensions although the TPEN-mediated fluorescence recovery was slower here, requiring almost 10 min compared to less than 1 min for full recovery in aerobic conditions. We also explored the ability of CreiLOV$_{N41C}$ to detect endogenous zinc under anaerobic conditions. As for the analogous aerobic experiment, *E. coli* cells were grown and expression was induced in the presence of varied $ZnCl_2$ concentrations (Figures 4D and S21). After anaerobic growth, cell suspensions were transferred to sealed cuvettes, and initial fluorescence was measured prior to the addition of TPEN and then Zn^{2+}/saponin/pyrithione. A comparison of the relative intensities shows that added $ZnCl_2$ up to 1.0 mM does not affect the initial fluorescence of CreiLOV$_{N41C}$, and minor effects were observed at 1.5 mM added $ZnCl_2$. When cells were grown and CreiLOV$_{N41C}$ expression induced in the presence of 2.0 mM $ZnCl_2$, endogenous zinc could be detected, as evidenced by an increase in fluorescence upon addition of TPEN. The Zn^{2+}-induced quenching and TPEN-mediated fluorescence recovery of CreiLOV$_{N41C}$ observed under both aerobic and anaerobic conditions for exogenous and endogenous zinc support its utility as an oxygen-independent metal sensor.

Metal Binding Site Analysis and Possible Metal-Induced Quenching Mechanisms for CreiLOV$_{N41C}$. Zinc and copper binding studies on CreiLOV and mutant CreiLOV proteins support the hypothesis that residues in positions 17 and 41 are involved in facilitating the metal-induced fluorescence quenching. For CreiLOV$_{N41C}$, the presence of both thiol residues (Cys17 and Cys41) leads to strong binding affinities and increased extent of fluorescence quenching by comparison to variants with one or no cysteine residues in the binding site (Figure 1).

The mechanism of fluorescence quenching is not identified in this work but may be considered. Copper-induced fluorescence quenching is a common occurrence for fluorescent proteins and can usually be attributed to static quenching, electron transfer, or energy transfer between a colored metal ion (i.e., Cu^{2+}) and the fluorophore.[59−62] Static quenching would require direct contact between the chromophore and quenching metal, and this is not supported by the spectroscopic results. The only change in the UV−visible spectrum at 270 nm (Figure S4) is likely due to the interaction between copper and the thiolate ligand.[31,32] Electron transfer usually occurs at short distances (<5 Å), and energy transfer such as from FRET has been observed between 7 and 20 Å in fluorescent proteins.[62] Here, the minimal distance between the modeled metal location and the flavin fluorophore is <5 Å. Energy transfer could also occur between metals with partially filled d-orbitals (i.e., Cu^{2+}) and a photoexcited ligand (flavin fluorescent protein) by a double electron exchange process called Dexter Energy Transfer.[2,63] This is a short-range mechanism that typically occurs at <10 Å and requires wave function overlap. Other mechanisms should be considered for metals with filled d-orbitals, like Zn^{2+} and Cu^{+}. Here, fluorescence enhancement is common and quenching rare, although it has been observed.[64,65] Zinc-induced quenching could occur by static quenching, as for Zn^{2+} binding to fluorescent tryptophan residues in proteins, but this is not supported by our spectroscopic data (Figure S4). Zinc may also quench protein fluorescence through conformational perturbations.[66,67]

https://doi.org/10.1021/acssensors.2c01376
ACS Sens. 2022, 7, 3369−3378

CONCLUSIONS

FbFPs are excellent candidates for designing new fluorescent protein-based metal ion sensors that do not require oxygen to become fluorescent. In this work, we have shown that single site-directed mutagenesis near the flavin site of CreiLOV leads to high affinity and reversible quenching by zinc ions. Furthermore, copper-induced quenching is retained in $CreiLOV_{N41C}$ with a several orders-of-magnitude stronger K_d for both copper(I) and copper(II) ions. Our data support a proposed metal ion binding site that includes amino acids at positions 17 and 41 along with the two oxygen atoms from the FMN cofactor. Using a series of mutants, $CreiLOV_{C17A}$, $CreiLOV_{N41D}$, and $CreiLOV_{N41C}$, we confirm that the residues in positions 17 and 41 impact metal-induced fluorescence quenching properties. Of these mutants, $CreiLOV_{N41C}$ exhibited significantly higher affinity (up to femtomolar compared to nanomolar K_d) and extent of quenching for $Cu^{+/2+}$ and was the only variant that could be reversibly quenched by Zn^{2+} ions. In live *E. coli* cells, $CreiLOV_{N41C}$ rapidly and reversibly responds to the addition of zinc ions over several cycles of chelator and zinc addition, whereas reversibility for copper is incomplete and over several cycles leads to significant loss of fluorescence. Although affinity for copper is high, the lack of complete reversibility limits application as a sensor in cells. On the other hand, $CreiLOV_{N41C}$ is a useful sensor for zinc given its rapid and reversible response to Zn^{2+} ions and its nanomolar K_d that falls into a physiologically relevant range for labile zinc in cells. Furthermore, reversible endogenous Zn^{2+}-induced fluorescence quenching can be detected in *E. coli* cells when grown in the presence of varied zinc in the medium. Analysis of the zinc sensitivity of $CreiLOV_{N41C}$ expressed in *E. coli* grown under anaerobic conditions strongly supports the utility of this mutant for imaging zinc fluctuations in anaerobic organisms, thus broadening the range of biological systems that can now be investigated using fluorescent protein-based zinc sensors.

EXPERIMENTAL SECTION

General Information. All reagents were purchased from commercial sources and used as received. *E. coli* strain MG1655 was from ATCC. *E. coli* strains DH5α and BL21(DE3) were obtained from New England Biolabs. UV−visible absorption spectra were obtained on an Agilent Cary 100 UV−visible spectrophotometer and fluorescence spectra on an Agilent Eclipse spectrofluorometer using quartz cuvettes (Starna cells) with 1 cm path lengths. All measurements were conducted at 25.0 °C, maintained by a circulating water bath. To remove the adventitious metal ions, all buffers for spectroscopy were treated with Chelex-100 resin (Bio-Rad) according to the manufacturer's batch protocol. Experiments involving $CreiLOV_{N41C}$ and Cu^+ were done anaerobically using buffer that was freshly degassed with argon. Anaerobic manipulations were done in an anaerobic chamber or using cuvettes with a screw cap and septum and a gas-tight Hamilton syringe. Fluorescence data was obtained by exciting at 450 nm. Excitation and emission slit widths were set to 5 nm and emission acquired from 470 to 600 nm.

Zinc and Copper Affinity Titrations. The dissociation constants of Zn^{2+} (for $CreiLOV_{N41C}$) and Cu^{2+} (for CreiLOV, $CreiLOV_{N41D}$, $CreiLOV_{C17A}$, and $CreiLOV_{N41C}$) were determined at pH 7.1. All titrations for $CreiLOV_{N41C}$ and all Cu^+ titrations for CreiLOV and CreiLOV mutants were done under anaerobic conditions by preparing samples in the anaerobic chamber and using a cuvette with septum. Cu^{2+} titrations were carried out with EDTA (1 mM, $CreiLOV_{N41C}$) or ADA (1 mM, CreiLOV, $CreiLOV_{N41D}$, or $CreiLOV_{C17A}$) to buffer Cu^{2+} concentrations. The Zn^{2+} titration for $CreiLOV_{N41C}$ was carried out with EGTA (1 mM). Free Zn^{2+} and Cu^{2+} concentrations were calculated with Maxchelator (Table S4). The dissociation constant of Cu^+ for $CreiLOV_{N41C}$ was determined at pH 7.3 and in the presence of GSH to buffer the Cu^+ concentration. Free Cu^+ concentrations were calculated using the binding affinity of GSH-Cu^+ ($K_d = 10^{-13.3}$ M, Table S4).[35] The Cu^+ binding affinities of CreiLOV, $CreiLOV_{N41D}$, and $CreiLOV_{C17A}$ were estimated by direct titration of $[Cu(CH_3CN)_4]PF_6$ with protein (3 μM) buffered at pH 7.1. For each titration, aliquots of metal were added to the protein. For each aliquot, the spectrum was recorded after incubating 1 min and ensuring equilibrium (no changes beyond 1 min were observed). Integrated fluorescence intensity (470 to 600 nm, normalized to initial protein fluorescence) was plotted against total metal concentration for each addition. The binding curves were fitted to a single site model (accounting for buffering chelator) for apparent K_d using DynaFit (http://www.biokin.com/dynafit/). Figure S22 shows an example fitting script.

Live Cell Suspension Assays for Metal Binding. The procedure for aerobic cell suspension experiments with $CreiLOV_{N41C}$ followed the previously published protocol for CreiLOV,[26] with changes to the medium and metals used as described in the Supporting Information. For anaerobic cell suspension assays, single colonies of *E. coli* MG1655 cells transformed with pQE80L-$CreiLOV_{N41C}$ were incubated in LB broth (100 mL) containing ampicillin (100 μg/mL) and grown overnight at 37 °C with shaking. The resulting culture was used to inoculate LB medium (1:100) containing glucose (20 mM), potassium nitrate (20 mM) as an electron acceptor, and ampicillin (100 μg/mL) to OD_{600} = 0.04 in a 100 mL glass bottle under anaerobic conditions. To maintain anaerobic conditions, the culture was degassed in an anaerobic chamber and sealed with screw cap and septum. Cells were grown statically at 37 °C to OD_{600} = 0.3 (∼1.5 h). $CreiLOV_{N41C}$ expression was induced with IPTG (0.5 mM), and cells were incubated at 37 °C for 3 h. A 2.5 mL portion of the expressed culture was harvested by pelleting cells and washing twice with PBS buffer (20 mM Na_2HPO_4, 200 mM NaCl, pH 8.0). For each sample, the following procedure was carried out: the cells were resuspended in 5 mL of metal-free HEPES buffer (50 mM HEPES, 100 mM NaCl, pH 7.1) containing EDTA (1 mM) in a 10 mL metal-free Falcon tube and incubated 10 min. The cells were pelleted by centrifugation, the supernatant was removed, and the cells were resuspended in 2.5 mL of HEPES buffer and transferred to a cuvette with screw cap and septum in the glovebox. With the sample constantly stirring, fluorescence was recorded. TPEN (50 μM) was added, and fluorescence was recorded at regular intervals for 1 min (after which no further changes were observed). $ZnCl_2$ (100 μM), saponin (0.001%), and pyrithione (0.75 μM) were then added, and fluorescence was recorded at regular intervals for 1 min (no changes were observed beyond this time frame). Digitonin did not permeabilize these cells well, but combined saponin and pyrithione yielded suitable results.[50] Lastly, TPEN (200 μM) was added, and the fluorescence was recorded at regular intervals for ∼10 min (after which no further changes were observed). Anaerobic conditions were maintained throughout using sealed flasks and cuvettes with septa and by performing manipulations within an anaerobic chamber or using a gas-tight Hamilton syringe. For endogenous zinc detection, starter cultures were inoculated into LB medium containing added $ZnCl_2$ (100 μM to 2 mM) and grown and induced as described above (anaerobic) and in the Supporting Information (aerobic). The cells were collected, washed, and resuspended as described, and then the initial fluorescence intensity was recorded, followed by the fluorescence intensity upon the addition of TPEN (50 μM) and then with the addition of Zn^{2+}/digitonin (100 μM/30 μM) for aerobic cultures or $ZnCl_2$/saponin/pyrithione for anaerobic cultures. $ZnCl_2$/saponin/pyrithione concentrations were 100 μM/0.001%/0.75 μM for 0.1 and 1.0 mM added $ZnCl_2$ conditions and 100 μM/0.002%/1.5 μM for 1.5 and 2.0 mM added $ZnCl_2$ conditions.

Fluorescence Microscopy Imaging of Live Bacterial Cells. *E. coli* BL21(DE3) cells transformed with pET28a-$CreiLOV_{N41C}$ were grown, and protein expression was induced as before. Cell pellets were then harvested, washed, and resuspended in metal-free HEPES buffer

https://doi.org/10.1021/acssensors.2c01376
ACS Sens. 2022, 7, 3369−3378

as described for live cell suspension assays. The cells were attached to a thin layer of 3% agarose on a general microscope slide by adding 5 μL of cell suspension and then placing a cover glass on top. Imaging experiments were performed using an ECHO Revolve microscope equipped with a 5 MP CMOS Monochrome Camera (Fluorescence) and 12 MP Color Camera. The light source was a LED light cube-FITC(M). Fluorescence images were obtained with an oil-immersion objective at 100× magnification. The exposure time, sensitivity, and contrast for acquisition of fluorescence images were kept constant for each series of images for each channel. Images were collected using the included software. Images were obtained by exciting at 470/40 nm. Both emission and brightfield images were obtained. Images were collected prior to and after the addition of TPEN (50 μM) and upon the addition of $ZnCl_2$/digitonin (100 μM/30 μM) to the cells. Lastly, TPEN (100 μM) was added to the cells, and images were recorded. Images were collected after 1 min incubation for each step. Longer incubations were tested but found not to be necessary. Images were analyzed with ImageJ (http://imagej.nih.gov/ij/). Each image was background corrected. Each bacterial cell was manually selected and the mean intensity measured by ImageJ. The background intensity was calculated by selecting regions of the image that did not have any cells and was subtracted from the cell values for each image. The mean intensity per cell was used to calculate the sensor intensity initially, with TPEN, with Zn^{2+}/digitonin, and with subsequent TPEN.

■ ASSOCIATED CONTENT

Supporting Information

The Supporting Information is available free of charge at https://pubs.acs.org/doi/10.1021/acssensors.2c01376.

Expanded experimental section, primers, additional characterizations of proteins, and DNA and protein sequences (PDF)

■ AUTHOR INFORMATION

Corresponding Author

Melissa L. Zastrow − *Department of Chemistry, University of Houston, Houston, Texas 77204, United States;* orcid.org/0000-0002-5910-6948; Email: mzastrow@central.uh.edu

Authors

Wenping Zou − *Department of Chemistry, University of Houston, Houston, Texas 77204, United States*

Hazel N. Nguyen − *Department of Chemistry, University of Houston, Houston, Texas 77204, United States*

Complete contact information is available at: https://pubs.acs.org/10.1021/acssensors.2c01376

Funding

This work was supported by The Welch Foundation grant E-1972 (M.L.Z.), NIH-NIGMS grant R35 GM138223 (M.L.Z.), and the University of Houston New Faculty Startup Grant (M.L.Z.).

Notes

The authors declare no competing financial interest.

■ ACKNOWLEDGMENTS

We would like to thank Prof. Arnab Mukherjee and Prof. Charles M. Schroeder for the plasmid pQE80L-CreiLOV; Prof. Thomas Teets (UH) for the use of his fluorometer and Sungwon Yoon (UH) for assistance with fluorescence lifetime experiments; and all members of the Zastrow group for valuable discussions.

■ REFERENCES

(1) Aggett, P. J. 1 Physiology and Metabolism of Essential Trace Elements: An Outline. *Clin. Endocrinol. Metab.* **1985**, *14*, 513−543.

(2) Carter, K. P.; Young, A. M.; Palmer, A. E. Fluorescent Sensors for Measuring Metal Ions in Living Systems. *Chem. Rev.* **2014**, *114*, 4564−4601.

(3) Bischof, H.; Burgstaller, S.; Waldeck-Weiermair, M.; Rauter, T.; Schinagl, M.; Ramadani-Muja, J.; Graier, W. F.; Malli, R. Live-Cell Imaging of Physiologically Relevant Metal Ions Using Genetically Encoded FRET-Based Probes. *Cells* **2019**, *8*, 492.

(4) Baek, K.; Ji, K.; Peng, W.; Liyanaarachchi, S. M.; Dodani, S. C. The Design and Evolution of Fluorescent Protein-Based Sensors for Monoatomic Ions in Biology. *Protein Eng., Des. Sel.* **2021**, *34*, gzab023.

(5) Sanford, L.; Palmer, A. Recent Advances in Development of Genetically Encoded Fluorescent Sensors. In *Enzymes as Sensors*; Thompson, R. B., Fierke, C. A., Eds.; Elsevier Inc., 2017; Vol. *589*, pp 1−49.

(6) Pratt, E. P. S.; Damon, L. J.; Anson, K. J.; Palmer, A. E. Tools and Techniques for Illuminating the Cell Biology of Zinc. *Biochim. Biophys. Acta Mol. Cell Res.* **2021**, *1868*, 118865.

(7) Tsien, R. Y. The Green Fluorescent Protein. *Annu. Rev. Biochem.* **1998**, *67*, 509−544.

(8) Remington, S. J. Fluorescent Proteins: Maturation, Photochemistry and Photophysics. *Curr. Opin. Struct. Biol.* **2006**, *16*, 714−721.

(9) Ozbakir, H. F.; Anderson, N. T.; Fan, K. C.; Mukherjee, A. Beyond the Green Fluorescent Protein: Biomolecular Reporters for Anaerobic and Deep-Tissue Imaging. *Bioconjugate Chem.* **2020**, *31*, 293−302.

(10) Chia, H. E.; Marsh, E. N. G.; Biteen, J. S. Extending Fluorescence Microscopy into Anaerobic Environments. *Curr. Opin. Chem. Biol.* **2019**, *51*, 98−104.

(11) Buckley, A. M.; Petersen, J.; Roe, A. J.; Douce, G. R.; Christie, J. M. LOV-Based Reporters for Fluorescence Imaging. *Curr. Opin. Chem. Biol.* **2015**, *27*, 39−45.

(12) Mukherjee, A.; Schroeder, C. M. Flavin-Based Fluorescent Proteins: Emerging Paradigms in Biological Imaging. *Curr. Opin. Biotechnol.* **2015**, *31*, 16−23.

(13) Christie, J. M.; Gawthorne, J.; Young, G.; Fraser, N. J.; Roe, A. J. LOV to BLUF: Flavoprotein Contributions to the Optogenetic Toolkit. *Mol. Plant* **2012**, *5*, 533−544.

(14) Drepper, T.; Eggert, T.; Circolone, F.; Heck, A.; Krauß, U.; Guterl, J.-K.; Wendorff, M.; Losi, A.; Gärtner, W.; Jaeger, K.-E. Reporter Proteins for in Vivo Fluorescence without Oxygen. *Nat. Biotechnol.* **2007**, *25*, 443−445.

(15) Chapman, S.; Faulkner, C.; Kaiserli, E.; Garcia-Mata, C.; Savenkov, E. I.; Roberts, A. G.; Oparka, K. J.; Christie, J. M. The Photoreversible Fluorescent Protein ILOV Outperforms GFP as a Reporter of Plant Virus Infection. *Proc. Natl. Acad. Sci. U.S.A.* **2008**, *105*, 20038−20043.

(16) Lobo, L. A.; Smith, C. J.; Rocha, E. R. Flavin Mononucleotide (FMN)-Based Fluorescent Protein (FbFP) as Reporter for Gene Expression in the Anaerobe Bacteroides Fragilis. *FEMS Microbiol. Lett.* **2011**, *317*, 67−74.

(17) Landete, J. M.; Langa, S.; Revilla, C.; Margolles, A.; Medina, M.; Arqués, J. L. Use of Anaerobic Green Fluorescent Protein versus Green Fluorescent Protein as Reporter in Lactic Acid Bacteria. *Appl. Microbiol. Biotechnol.* **2015**, *99*, 6865−6877.

(18) Landete, J. M.; Peirotén, Á.; Rodríguez, E.; Margolles, A.; Medina, M.; Arqués, J. L. Anaerobic Green Fluorescent Protein as a Marker of Bifidobacterium Strains. *Int. J. Food Microbiol.* **2014**, *175*, 6−13.

(19) Buckley, A. M.; Jukes, C.; Candlish, D.; Irvine, J. J.; Spencer, J.; Fagan, R. P.; Roe, A. J.; Christie, J. M.; Fairweather, N. F.; Douce, G. R. Lighting Up Clostridium Difficile: Reporting Gene Expression Using Fluorescent Lov Domains. *Sci. Rep.* **2016**, *6*, 23463.

(20) Walter, J.; Hausmann, S.; Drepper, T.; Puls, M.; Eggert, T.; Dihné, M. Flavin Mononucleotide-Based Fluorescent Proteins

Function in Mammalian Cells without Oxygen Requirement. *PLoS One* **2012**, *7*, No. e43921.
(21) Choi, C. H.; DeGuzman, J. V.; Lamont, R. J.; Yilmaz, Ö. Genetic Transformation of an Obligate Anaerobe, P. Gingivalis for FMN-Green Fluorescent Protein Expression in Studying Host-Microbe Interaction. *PLoS One* **2011**, *6* (). DOI: 10.1371/journal.-pone.0018499
(22) Mukherjee, A.; Weyant, K. B.; Agrawal, U.; Walker, J.; Cann, I. K. O.; Schroeder, C. M. Engineering and Characterization of New LOV-Based Fluorescent Proteins from *Chlamydomonas Reinhardtii* and *Vaucheria Frigida*. *ACS Synth. Biol.* **2015**, *4*, 371−377.
(23) Ravikumar, Y.; Nadarajan, S. P.; Lee, C. S.; Rhee, J. K.; Yun, H. A New-Generation Fluorescent-Based Metal Sensor - ILOV Protein. *J. Microbiol. Biotechnol.* **2015**, *25*, 503−510.
(24) Ravikumar, Y.; Nadarajan, S. P.; Lee, C.-S.; Jung, S.; Bae, D.-H.; Yun, H. FMN-Based Fluorescent Proteins as Heavy Metal Sensors Against Mercury Ions. *J. Microbiol. Biotechnol.* **2016**, *26*, 530−539.
(25) Ravikumar, Y.; Nadarajan, S.; Lee, C.; Yun, H. Engineering an FMN-Based ILOV Protein for the Detection of Arsenic Ions. *Anal. Biochem.* **2017**, *525*, 38−43.
(26) Zou, W.; Le, K.; Zastrow, M. L. Live-Cell Copper-Induced Fluorescence Quenching of the Flavin-Binding Fluorescent Protein CreiLOV. *ChemBioChem* **2020**, *21*, 1356−1363.
(27) Zhao, H.; Zastrow, M. L. Transition Metals Induce Quenching of Monomeric Near-Infrared Fluorescent Proteins. *Biochemistry* **2022**, *61*, 494−504.
(28) Reyes-Caballero, H.; Campanello, G. C.; Giedroc, D. P. Metalloregulatory Proteins: Metal Selectivity and Allosteric Switching. *Biophys. Chem.* **2011**, *156*, 103−114.
(29) Braymer, J. J.; Giedroc, D. P. Recent Developments in Copper and Zinc Homeostasis in Bacterial Pathogens. *Curr. Opin. Chem. Biol.* **2014**, *19*, 59−66.
(30) Wang, D.; Hosteen, O.; Fierke, C. a. ZntR-Mediated Transcription of ZntA Responds to Nanomolar Intracellular Free Zinc. *J. Inorg. Biochem.* **2012**, *111*, 173−181.
(31) Wegner, S. V.; Arslan, H.; Sunbul, M.; Yin, J.; He, C. Dynamic Copper(I) Imaging in Mammalian Cells with a Genetically Encoded Fluorescent Copper(I) Sensor. *J. Am. Chem. Soc.* **2010**, *132*, 2567−2569.
(32) Pountney, D. L.; Schauwecker, I.; Zarn, J.; Vasak, M. Formation of Mammalian Cu8-Metallothionein in Vitro: Evidence for the Existence of Two Cu(I)4-Thiolate Clusters. *Biochemistry* **1994**, *33*, 9699−9705.
(33) Schafer, F. Q.; Buettner, G. R. Redox Environment of the Cell as Viewed through the Redox State of the Glutathione Disulfide/Glutathione Couple. *Free Radic. Biol. Med.* **2001**, *30*, 1191−1212.
(34) Trachootham, D.; Lu, W.; Ogasawara, M. A.; Valle, N. R.-d.; Huang, P. Redox Regulation of Cell Survival. *Antioxid. Redox Signaling* **2008**, *10*, 1343−1374.
(35) Xiao, Z.; Brose, J.; Schimo, S.; Ackland, S. M.; La Fontaine, S.; Wedd, A. G. Unification of the Copper(I) Binding Affinities of the Metallo-Chaperones Atx1, Atox1, and Related Proteins: Detection Probes and Affinity Standards. *J. Biol. Chem.* **2011**, *286*, 11047−11055.
(36) Hessels, A. M.; Merkx, M. Genetically-Encoded FRET-Based Sensors for Monitoring Zn^{2+} in Living Cells. *Metallomics* **2015**, *7*, 258−266.
(37) Qiao, W.; Mooney, M.; Bird, A. J.; Winge, D. R.; Eide, D. J. Zinc Binding to a Regulatory Zinc-Sensing Domain Monitored in Vivo by Using FRET. *Proc. Natl. Acad. Sci. U.S.A.* **2006**, *103*, 8674−8679.
(38) van Dongen, E. M. W. M.; Dekkers, L. M.; Spijker, K.; Meijer, E. W.; Klomp, L. W. J.; Merkx, M. Ratiometric Fluorescent Sensor Proteins with Subnanomolar Affinity for Zn(II) Based on Copper Chaperone Domains. *J. Am. Chem. Soc.* **2006**, *128*, 10754−10762.
(39) van Dongen, E. M. W. M.; Evers, T. H.; Dekkers, L. M.; Meijer, E. W.; Klomp, L. W. J.; Merkx, M. Variation of Linker Length in Ratiometric Fluorescent Sensor Proteins Allows Rational Tuning of Zn(II) Affinity in the Picomolar to Femtomolar Range. *J. Am. Chem. Soc.* **2007**, *129*, 3494−3495.
(40) Vinkenborg, J. L.; Nicolson, T. J.; Bellomo, E. A.; Koay, M. S.; Rutter, G. A.; Merkx, M. Genetically Encoded FRET Sensors to Monitor Intracellular Zn^{2+} Homeostasis. *Nat. Methods* **2009**, *6*, 737−740.
(41) Dittmer, P. J.; Miranda, J. G.; Gorski, J. A.; Palmer, A. E. Genetically Encoded Sensors to Elucidate Spatial Distribution of Cellular Zinc. *J. Biol. Chem.* **2009**, *284*, 16289−16297.
(42) Qin, Y.; Dittmer, P. J.; Park, J. G.; Jansen, K. B.; Palmer, A. E. Measuring Steady-State and Dynamic Endoplasmic Reticulum and Golgi Zn^{2+} with Genetically Encoded Sensors. *Proc. Natl. Acad. Sci. U.S.A.* **2011**, *108*, 7351−7356.
(43) Hessels, A. M.; Chabosseau, P.; Bakker, M. H.; Engelen, W.; Rutter, G. A.; Taylor, K. M.; Merkx, M. EZinCh-2: A Versatile, Genetically Encoded FRET Sensor for Cytosolic and Intraorganelle Zn^{2+} Imaging. *ACS Chem. Biol.* **2015**, *10*, 2126−2134.
(44) Koay, M. S.; Janssen, B. M. G.; Merkx, M. Tuning the Metal Binding Site Specificity of a Fluorescent Sensor Protein: From Copper to Zinc and Back. *Dalton Trans.* **2013**, *42*, 3230−3232.
(45) Qin, Y.; Sammond, D. W.; Braselmann, E.; Carpenter, M. C.; Palmer, A. E. Development of an Optical Zn^{2+} Probe Based on a Single Fluorescent Protein. *ACS Chem. Biol.* **2016**, *11*, 2744−2751.
(46) Chen, Z.; Ai, H. Single Fluorescent Protein-Based Indicators for Zinc Ion (Zn^{2+}). *Anal. Chem.* **2016**, *88*, 9029−9036.
(47) Chen, M.; Zhang, S.; Xing, Y.; Li, X.; He, Y.; Wang, Y.; Oberholzer, J.; Ai, H. W. Genetically Encoded, Photostable Indicators to Image Dynamic Zn2+ Secretion of Pancreatic Islets. *Anal. Chem.* **2019**, *91*, 12212−12219.
(48) Fudge, D. H.; Black, R.; Son, L.; LeJeune, K.; Qin, Y. Optical Recording of Zn 2+ Dynamics in the Mitochondrial Matrix and Intermembrane Space with the GZnP2 Sensor. *ACS Chem. Biol.* **2018**, *13*, 1897−1905.
(49) Wu, T.; Kumar, M.; Zhao, S.; Drobizhev, M.; Tian, X.; Tzounopoulos, T.; Ai, H. A Genetically Encoded Far-Red Fluorescent Indicator for Imaging Synaptically-Released Zn2+. bioRxiv:2022.06.02.494512, **2022**.
(50) Carter, K. P.; Carpenter, M. C.; Fiedler, B.; Jimenez, R.; Palmer, A. E. Critical Comparison of FRET-Sensor Functionality in the Cytosol and Endoplasmic Reticulum and Implications for Quantification of Ions. *Anal. Chem.* **2017**, *89*, 9601−9608.
(51) Hötzer, B.; Ivanov, R.; Altmeier, S.; Kappl, R.; Jung, G. Determination of copper(II) ion concentration by lifetime measurements of green fluorescent protein. *J. Fluoresc.* **2011**, *21*, 2143−2153.
(52) Bálint, E.-É.; Petres, J.; Szabó, M.; Orbán, C. K.; Szilágyi, L.; Ábrahám, B. Fluorescence of a Histidine-Modified Enhanced Green Fluorescent Protein (EGFP) Effectively Quenched by Copper(II) Ions. *J. Fluoresc.* **2013**, *23*, 273−281.
(53) Eli, P.; Chakrabartty, A. Variants of DsRed Fluorescent Protein: Development of a Copper Sensor. *Protein Sci.* **2006**, *15*, 2442−2447.
(54) Rahimi, Y.; Goulding, A.; Shrestha, S.; Mirpuri, S.; Deo, S. K. Mechanism of Copper Induced Fluorescence Quenching of Red Fluorescent Protein, DsRed. *Biochem. Biophys. Res. Commun.* **2008**, *370*, 57−61.
(55) Rahimi, Y.; Shrestha, S.; Banerjee, T.; Deo, S. K. Copper Sensing Based on the Far-Red Fluorescent Protein, HcRed, from Heteractis Crispa. *Anal. Biochem.* **2007**, *370*, 60−67.
(56) Rigo, A.; Corazza, A.; Luisa di Paolo, M.; Rossetto, M.; Ugolini, R.; Scarpa, M. Interaction of Copper with Cysteine: Stability of Cuprous Complexes and Catalytic Role of Cupric Ions in Anaerobic Thiol Oxidation. *J. Inorg. Biochem.* **2004**, *98*, 1495−1501.
(57) Wingen, M.; Potzkei, J.; Endres, S.; Casini, G.; Rupprecht, C.; Fahlke, C.; Krauss, U.; Jaeger, K. E.; Drepper, T.; Gensch, T. The Photophysics of LOV-Based Fluorescent Proteins–New Tools for Cell Biology. *Photochem. Photobiol. Sci.* **2014**, *13*, 875−883.
(58) Homans, R. J.; Khan, R. U.; Andrews, M. B.; Kjeldsen, A. E.; Natrajan, L. S.; Marsden, S.; McKenzie, E. A.; Christie, J. M.; Jones, A. R. Two Photon Spectroscopy and Microscopy of the Fluorescent

Flavoprotein, ILOV. *Phys. Chem. Chem. Phys.* **2018**, *20*, 16949−16955.
(59) Lakowicz, J. R. *Principles of Fluorescence Spectroscopy*, 3rd ed.; Springer: New York, 2006.
(60) Richmond, T. a.; Takahashi, T. T.; Shimkhada, R.; Bernsdorf, J. Engineered Metal Binding Sites on Green Fluorescence Protein. *Biochem. Biophys. Res. Commun.* **2000**, *268*, 462−465.
(61) Isarankura-Na-Ayudhya, C.; Tantimongcolwat, T.; Galla, H. J.; Prachayasittikul, V. Fluorescent Protein-Based Optical Biosensor for Copper Ion Quantitation. *Biol. Trace Elem. Res.* **2010**, *134*, 352−363.
(62) Yu, X.; Strub, M. P.; Barnard, T. J.; Noinaj, N.; Piszczek, G.; Buchanan, S. K.; Taraska, J. W. An Engineered Palette of Metal Ion Quenchable Fluorescent Proteins. *PLoS One* **2014**, *9*, No. e95808.
(63) Dexter, D. L. A Theory of Sensitized Luminescence in Solids. *J. Chem. Phys.* **1953**, *21*, 836−850.
(64) Diana, R.; Panunzi, B. The Role of Zinc(II) Ion in Fluorescence Tuning of Tridentate Pincers: A Review. *Molecules* **2020**, *25* (). DOI: 10.3390/molecules25214984
(65) Barondeau, D. P.; Kassmann, C. J.; Tainer, J. A.; Getzoff, E. D. Structural Chemistry of a Green Fluorescent Protein Zn Biosensor. *J. Am. Chem. Soc.* **2002**, *124*, 3522−3524.
(66) Wu, M. X.; Filley, S. J.; Hill, K. A. W. Cooperative Binding of Zinc to an Aminoacyl-TRNA Synthetase. *Biochem. Biophys. Res. Commun.* **1994**, *201*, 1079−1083.
(67) Bernardo, M. M.; Day, D. E.; Halvorson, H. R.; Olson, S. T.; Shore, J. D. Surface-Independent Acceleration of Factor XII Activation by Zinc Ions. II. Direct Binding and Fluorescence Studies. *J. Biol. Chem.* **1993**, *268*, 12477−12483.

https://doi.org/10.1021/acssensors.2c01376
ACS Sens. 2022, 7, 3369−3378